PCCP

RSC Publishing

COMMUNICATION

Nanoporous silicon networks as anodes for lithium ion batteries

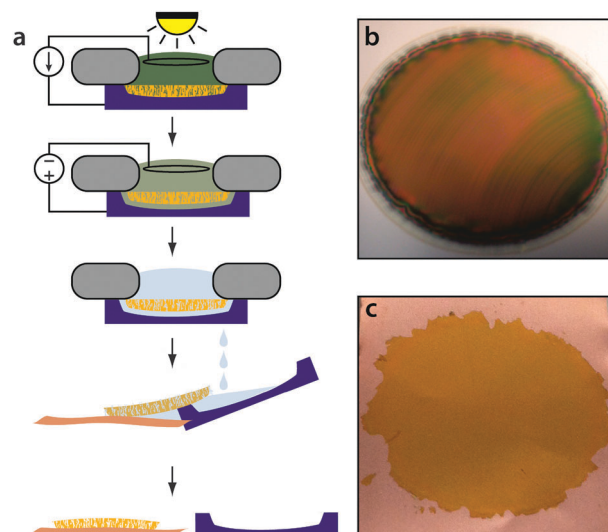Jia Zhu,[†][a] Christopher Gladden,[†][a] Nian Liu,[b] Yi Cui[b] and Xiang Zhang*[a]

Nanoporous silicon (Si) networks with controllable porosity and thickness are fabricated by a simple and scalable electrochemical process, and then released from Si wafers and transferred to flexible and conductive substrates. These nanoporous Si networks serve as high performance Li-ion battery electrodes, with an initial discharge capacity of 2570 mA h g^{-1}, above 1000 mA h g^{-1} after 200 cycles without any electrolyte additives.

Rechargeable lithium-ion batteries hold great promise as energy storage devices to solve the temporal and geographical mismatch between the supply and demand of electricity, and are therefore critical for many applications such as portable electronics and electric vehicles. Electrodes in these batteries are based on intercalation reactions in which Li$^+$ ions are inserted (extracted) from an open host structure with electron injection (removal).[1–4] However, the current electrode materials have limited specific charge storage capacity and cannot achieve the higher energy density, higher power density, and longer lifespan that all these important applications require.[3] Si as an alloying electrode material is attracting much attention because it has the highest known theoretical charge capacity (4200 mA h g^{-1}). However, it is challenging to overcome the issues associated with alloying and conversion reactions, which involve large structure and volume changes (400% volume expansion for Si) during Li$^+$ ion insertion and extraction. These issues can cause large hysteresis in the charge and discharge potentials, low power rate, and short cycle life, due to material instability, and poor electron and ion conduction.[5]

Recently, Si nanostructures have been intensively explored to attack the volume expansion and fracture problem.[6–16] For example, many Si nanostructures, such as Si nanowires,[6] carbon/Si spheres,[9] Si nanotubes,[17,18] core–shell crystalline/amorphous

Si nanowires,[19] Si nanotubes, have also shown initial capacity close to the theoretical limit, good (>90%) capacity retention over a large number of cycles.[20] However, low cost and fast throughput processes with great mass and morphology control are still desirable to reach the full potential for commercialization. Here we developed a simple and scalable electrochemical process to fabricate nanoporous Si networks with controllable porosity, which demonstrated a high initial discharge capacity of 2570 mA h g^{-1} and 200 cycles in electrochemical tests. Even after 200 cycles, this nanoporous Si network shows a capacity of above 1000 mA h g^{-1}. Good rate capability is demonstrated as well.

The nanoporous Si networks can be fabricated using a simple and scalable process (Fig. 1). Silicon wafer chips (0.01–0.02 Ω cm p-type) are secured in a Teflon etch cell filled with a 1 : 3 hydrofluoric acid and ethanol mixture. A nanoporous Si thin

[a] *NSF Nano-scale Science and Engineering Center (NSEC), 3112 Etcheverry Hall, University of California at Berkeley, Berkeley, California 94720, USA. E-mail: xiang@berkeley.edu*
[b] *Department of Materials Science and Engineering, Stanford University, Stanford, CA 94305, USA*
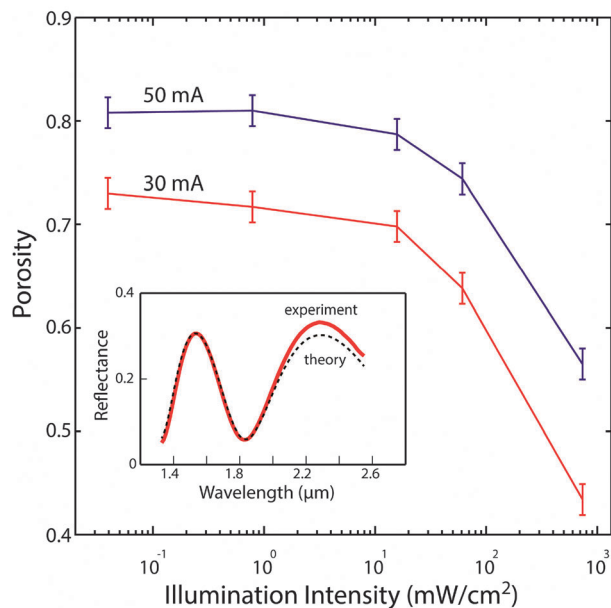† These authors contributed equally to this work.

Fig. 1 (a) Schematics of fabrication process flow. The nanoporous film is first etched in 3 : 1 HF : EtOH under illumination, then undercut in 20 : 1 HF : EtOH. After being rinsed in EtOH it can be transferred to Cu foil and the substrate is reused. (b) Nanoporous Si film on a Si substrate. (c) Nanoporous Si film transferred to a Cu film.

Fig. 2 The dependence of porosity on illumination intensity. Inset: Fourier transform infrared spectroscopy for porosity characterization.

film is etched under constant current and light illumination. Subsequently the solution is exchanged for 1 : 20 HF : EtOH and etched at 30 V to undercut the porous network and release it from the silicon substrate.[21] Finally the etch cell is flushed with pure ethanol, and then the thin layer of nanoporous Si is transferred to the Cu foil by slowly flowing ethanol over the chip while holding it in contact with the foil. The porous layer on the Cu foil is then rinsed with hexane and allowed to air dry. The silicon substrate can be reused many times, ensuring efficient use of the Si source material.

The porosity of these nanoporous Si networks can be controlled by adjusting the etching current and illumination intensity (Fig. 2). Increasing etching current uniformly increases the porosity of the network, while increasing illumination intensity decreases the porosity of the network.[22] The porosity is measured using FTIR reflectance spectroscopy which is then fitted using the dispersion of silicon and effective medium theory to calculate the refractive index and corresponding porosity[23] (Fig. 2, inset). We assume that the porosity is uniform along the thickness direction, which can be seen in Fig. 3b and e. To increase the accuracy of the model, the layer thickness is measured using SEM cross-section and compared to the model fitting.

To investigate the electrochemical performance of these nanoporous Si networks, two-electrode 2032 coin cells with these nanoporous Si networks (~ 20 nm pore size) on the Cu substrate were fabricated with Li metal as the counter electrode. As the volume of Si will expand upon the full lithiation to 400% of the original, it has been predicted and generally accepted that Si can only take around 20% in volume in order to have a good cyclability.[9] Therefore samples with 80% porosity, *i.e.* Si takes 20% of volume, were used in this study. To understand the intrinsic properties of these nanoporous Si networks, galvanostatic cycling was used with voltage cutoffs of 0.01 and 1 V *vs.* Li/Li^{+}. The charge capacity referred to here is the total charge inserted per unit mass of the nanoporous Si networks during Li insertion, whereas the discharge capacity is the total charge removed during Li extraction.

The structural changes of the nanoporous Si networks before and after lithiation were studied using scanning electron microscopy (SEM), and transmission electron microscopy (TEM).
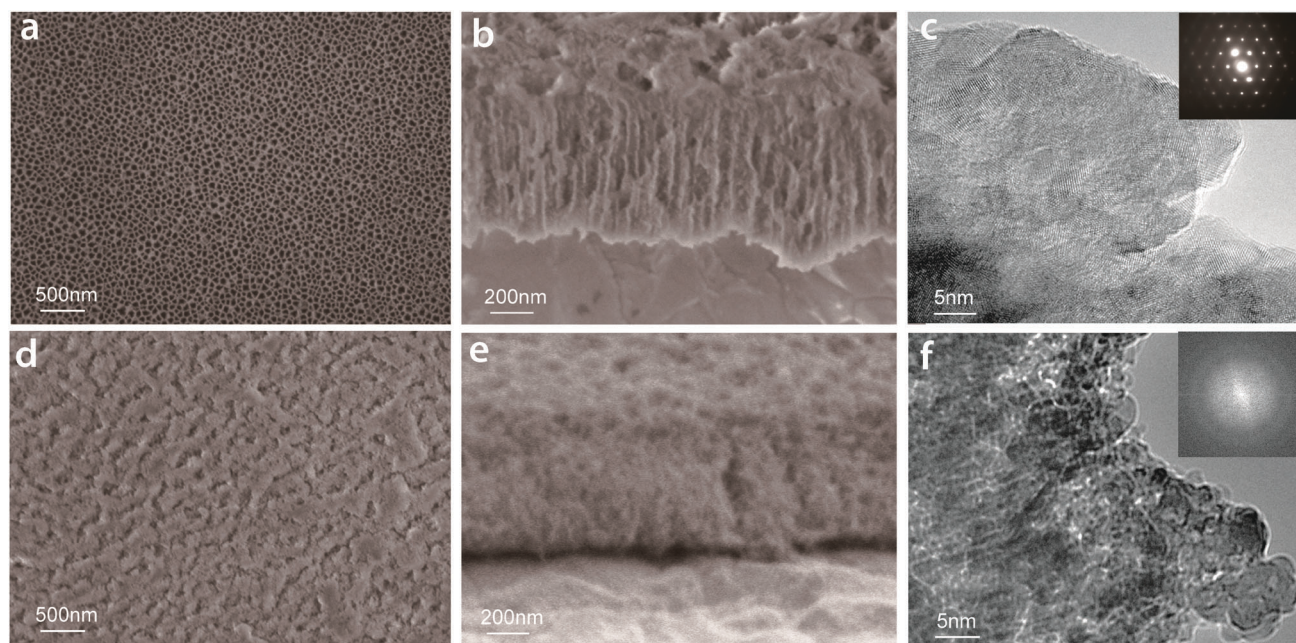
Fig. 3 Nanoporous Si networks before cycling (a) top view SEM image, (b) cross section SEM image, (c) TEM image, inset: SAD pattern. Nanoporous Si networks (SEI has been removed) after cycling (d) top view SEM image, (e) cross section SEM image, (f) TEM image, inset: SAD pattern.
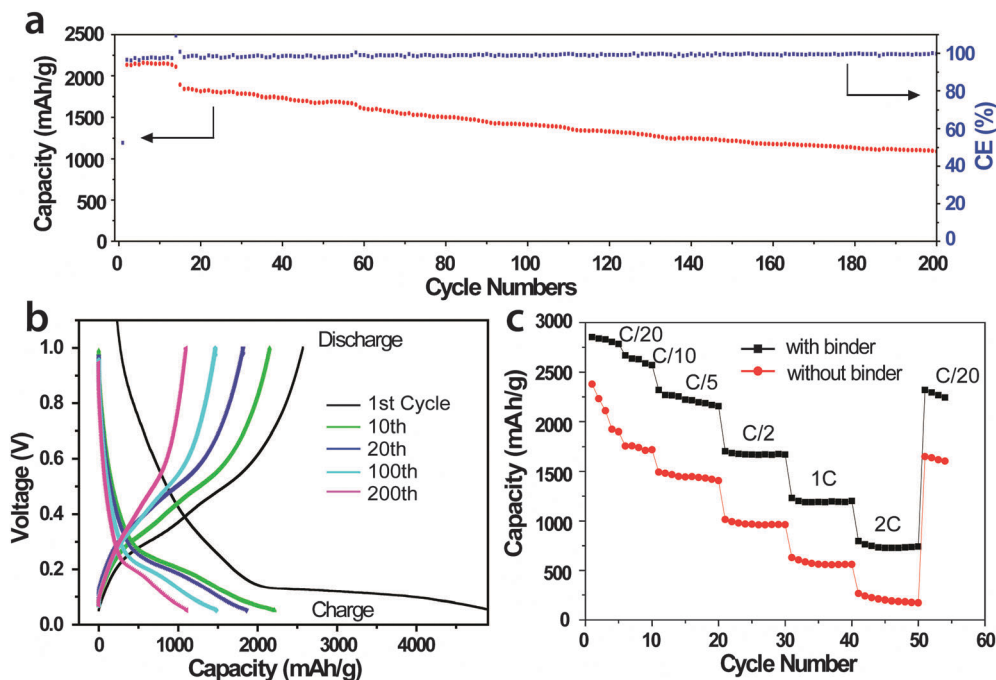
Fig. 4 Electrochemical characteristics of nanoporous Si networks tested between 1 V and 0.01 V. (a) Delithiation capacity and CE of nanoporous Si networks at the charge–discharge rate of C/10 for the first 15 cycles, then at the charge–discharge rate of 1 C until 200 cycles. (b) Voltage profiles plotted for the 1st, 10th, 20th, 100th and 200th cycles. (c) Capacity of nanoporous Si networks cycled at various rates from C/20 to 2 C. All the specific capacities of DWSiNTs are reported based on the total weight of Si–SiO$_x$.

The as-fabricated nanoporous Si networks have an average pore size of 20 nm and 1 μm thickness as revealed in the SEM image (Fig. 3a). Cross-section SEM showed that the whole porous Si networks are in good contact with the Cu substrate (Fig. 3b), which is crucial for battery performance. The as-fabricated nanoporous Si networks were single crystalline, as confirmed by TEM (Fig. 3c). As shown in Fig. 3f, the nanoporous Si becomes predominately amorphous during electrochemical cycling, similar to what has been observed in SiNWs. SEM (Fig. 3e) studies found that the networks remained adhered to the substrate. The pore size of the networks also appears to have decreased after lithiation, as expected from the predicted volume change. It is important to note that the networks do not pulverize after cycling because of the large porosity which can accommodate the volume change, as shown in Fig. 3d and e.

The first discharge capacity was 2570 mA h g^{-1} at the C/10 rate, or 10 h per half-cycle (Fig. 2). The irreversible capacity loss is likely due to reactions at the surface of these nanoporous structures. One possibility is the formation of a surface–electrolyte interphase (SEI) film due to electrolyte decomposition.[20,24,25] This has been well studied in both carbonaceous and Si electrodes. The second possibility is the decomposition of the native oxide that forms on the Si. The low Coulombic efficiency is limited to the first cycle, suggesting that any surface reactions occur only during the initial cycling. More studies will be done to determine the exact processes and the origin of the large initial irreversible capacity loss. The Coulombic efficiency starting from for the 2nd cycle is above 97%, showing good

reversible cycling after the surface reactions are completed. The discharge capacity remains stable at 1800 mA h g^{-1} over 20 cycles (Fig. 4a), indicating that the nanoporous Si networks remain in contact with the current collector and do not undergo pulverization.

The voltage profiles of the different cycles are shown in Fig. 4b. The lithiation potential shows a sloping profile between 0.1 and 0.01 V, consistent with the behaviour of amorphous silicon. No obvious change in the charge–discharge profile can be found after 200 cycles, indicating good cycling performance. This long cycle life without any electrolyte additive can be attributed to the stable SEI and the nanoporous Si materials.

High rate capabilities were also observed in the nanoporous Si networks (Fig. 4c). Charging–discharging at C/20, C/10, C/5, C/2, 1 C and 2 C revealed good cyclability. The Coulombic efficiency of 99.7% was also quite high, indicating good reversibility. The capacity was very stable at the high rates, indicating good Li diffusivity in the Si. Although the capacity dropped at the 1 C rate to 1200 mA h g^{-1}, it was still much higher than the theoretical capacity of graphite (372 mA h g^{-1}). Also it is found that addition of a binder (CMC binder) can improve the performance, which has been reported before.[16] In the case of the Si–C composite, it is reported that the addition of a binder can improve the performance by holding the active materials together.[7] However, in this study, since the nanoporous Si networks did not pulverize after electrochemical cycling, it is believed that the binder improves the performance by improving the electrical contact between active materials and current collectors.

442 | *Phys. Chem. Chem. Phys.*, 2013, **15**, 440–443

This journal is © the Owner Societies 2013

Conclusion

In conclusion, we have shown that nanoporous Si network anodes with 80% porosity have a high specific capacity (2570 mA h g^{-1}) and good cycling performance (>200 cycles) without any electrolyte additives. Our nanoporous Si anode design is easy to fabricate and has good electronic contact between the network and the current collector. Thus, nanoporous Si networks can be a promising, higher-capacity alternative for the existing graphite anode in Li ion batteries.

Acknowledgements

Notes and references

1 J. B. Goodenough and Y. Kim, *Chem. Mater.*, 2009, **22**, 587–603.
2 M. S. Whittingham, *ChemInform*, 2004, **35**, 4271.
3 M. Armand and J. M. Tarascon, *Nature*, 2008, **451**, 652–657.
4 J. M. Tarascon and M. Armand, *Nature*, 2001, **414**, 359–367.
5 W.-J. Zhang, *J. Power Sources*, 2011, **196**, 13–24.
6 C. K. Chan, H. Peng, G. Liu, K. McIlwrath, X. F. Zhang, R. A. Huggins and Y. Cui, *Nat. Nanotechnol.*, 2008, **3**, 31–35.
7 A. Magasinski, P. Dixon, B. Hertzberg, A. Kvit, J. Ayala and G. Yushin, *Nat. Mater.*, 2010, **9**, 353–358.
8 N. Liu, H. Wu, M. T. McDowell, Y. Yao, C. Wang and Y. Cui, *Nano Lett.*, 2012, **12**, 3315–3321.
9 S. D. Beattie, D. Larcher, M. Morcrette, B. Simon and J.-M. Tarascon, *J. Electrochem. Soc.*, 2008, **155**, A158–A163.
10 X.-W. Zhang, P. K. Patil, C. Wang, A. J. Appleby, F. E. Little and D. L. Cocke, *J. Power Sources*, 2004, **125**, 206–213.
11 L. A. Riley, A. S. Cavanagh, S. M. George, Y. S. Jung, Y. Yan, S.-H. Lee and A. C. Dillon, *ChemPhysChem*, 2010, **11**, 2124–2130.
12 M. Thakur, M. Isaacson, S. L. Sinsabaugh, M. S. Wong and S. L. Biswal, *J. Power Sources*, 2012, **205**, 426–432.
13 Y. Zhao, X. Liu, H. Li, T. Zhai and H. Zhou, *Chem. Commun.*, 2012, **48**, 5079–5081.
14 M. Ge, J. Rong, X. Fang and C. Zhou, *Nano Lett.*, 2012, **12**, 2318–2323.
15 I. Kovalenko, B. Zdyrko, A. Magasinski, B. Hertzberg, Z. Milicev, R. Burtovyy, I. Luzinov and G. Yushin, *Science*, 2011, **334**, 75–79.
16 D. Mazouzi, B. Lestriez, L. Roué and D. Guyomard, *Electrochem. Solid-State Lett.*, 2009, **12**, A215–A218.
17 T. Song, J. Xia, J.-H. Lee, D. H. Lee, M.-S. Kwon, J.-M. Choi, J. Wu, S. K. Doo, H. Chang, W. I. Park, D. S. Zang, H. Kim, Y. Huang, K.-C. Hwang, J. A. Rogers and U. Paik, *Nano Lett.*, 2010, **10**, 1710–1716.
18 M.-H. Park, M. G. Kim, J. Joo, K. Kim, J. Kim, S. Ahn, Y. Cui and J. Cho, *Nano Lett.*, 2009, **9**, 3844–3847.
19 L.-F. Cui, R. Ruffo, C. K. Chan, H. Peng and Y. Cui, *Nano Lett.*, 2008, **9**, 491–495.
20 H. Wu, G. Chan, J. W. Choi, I. Ryu, Y. Yao, M. T. McDowell, S. W. Lee, A. Jackson, Y. Yang, L. Hu and Y. Cui, *Nat. Nanotechnol.*, 2012, **7**, 310–315.
21 Y. Kanemitsu, H. Uto, Y. Masumoto, T. Matsumoto, T. Futagi and H. Mimura, *Phys. Rev. B: Condens. Matter Mater. Phys.*, 1993, **48**, 2827–2830.
22 C. Levy-Clement, A. Lagoubi, R. Tenne and M. Neumann-Spallart, *Electrochim. Acta*, 1992, **37**, 877–888.
23 K. Vanga, D. Cheam, C. Middlebrook and P. Bergstrom, *Phys. Status Solidi C*, 2011, **8**, 1941–1945.
24 D. Aurbach, *J. Power Sources*, 2000, **89**, 206–218.
25 P. Verma, P. Maire and P. Novák, *Electrochim. Acta*, 2010, **55**, 6332–6341.